# Extended Transfer Bound Error Analysis for Parametric Channel with Continuous Valued Correlated Random Nuisance Parameter

*Jan VČELÁK, Jan SÝKORA*

Dept. of Radioelectronics, Czech Technical University in Prague, Technická 2, 166 27 Praha, Czech Republic

vcelakj@fel.cvut.cz, jan.sykora@fel.cvut.cz

**Abstract.** *In this paper we address the extended use of transfer bound analysis of bit error rate (BER) properties. In conjunction with proper parameter modeling, we offer a method to resolve the problem of transfer bound applicability on a system with random and possibly correlated* continuous valued *nuisance parameters. We introduce a new additional parameter space into the original error space and join them in a product matrix for an extended transfer function evaluation. Example applications with simple trellis code for Rayleigh fading channel and phase synchronization error are investigated to demonstrate the functionality of the proved principle. Computer simulation results are presented for two different codes and various fading scenarios, and comparisons are made among analytical and measured system error performances.*

## Keywords

BER analysis, Transfer bound, Channel nuisance parameters, Markov models.

## 1. Introduction

The true BER performance analysis of arbitrary detector needs to evaluate all transition probabilities, which is possible only for elementary cases of communication systems. That is the reason, why approximate approaches through pairwise error probability and union bounding technique come into our consideration [3]. However, the price generally paid is expected error at low signal to noise ratios (SNR), which potentially limit success in bounding of concatenated codes. Among all concatenated blocks the system with a finite memory, whose transitions are determined by input sequences in finite trellis is of concern. Both the code and an optimum decoder are expected to have the same state description. Optimum detector then makes an error event, when he starts to follow the different path from the encoder. Where the brute force search for moderate number of such error events is not numerically tractable, transfer bound (TB) offers a partial solution [4]. TB models an error system as a finite state machine (FSM) and applies the results from FSM theory to searching in its probabilistic state diagram. This work is a follow-up to our recent conference paper [1]. It was necessary to extend our results to the applications in more realistic scenarios including phase estimation error and build the solid background to the problem.

We are now confronted with a problem of error analysis of a communication system with a finite memory and additional *continuous valued parameters*. Such situation can be normally found in a communication system, which operates through a wireless channel. The channel impairs output symbols by series of nuisance parameters, which could be deterministic or random. For random ones their statistical behavior in time and realizations must be considered in performance analysis. Thus we are mainly focused on adopting TB method to be able to cope with time dependant continuous valued random parameter. Our proposed solution is based on a suitable parameter modeling and presents a general framework for error analysis of finite memory modulation and random continuous correlated nuisance parameters.

At the beginning the paper shows essential prerequisites to TB analysis and FSM theory. The next section is devoted to the definition of the main concepts and quantities, from parameter modeling to extended TB. Section 4 shows an application of the proved principles into performance analysis of a real communication system.

## 2. Union Bound

Following [5], the probability of the first error event is easily evaluated as

$$P(e) \leq \sum_{\check{\mathbf{t}}_e} p(\check{\mathbf{t}}_e) \sum_{\check{\mathbf{t}}_d : \check{\mathbf{t}}_d \neq \check{\mathbf{t}}_e} \Pr\left(\check{\mathbf{t}}_d \left| \check{\mathbf{t}}_e \right.\right) \quad (1)$$

where $\check{\mathbf{t}}_e$ and $\check{\mathbf{t}}_d$ are hypothesized sequences of correct encoder and incorrect decoder state transitions. The $\Pr\left(\check{\mathbf{t}}_d \left| \check{\mathbf{t}}_e \right.\right)$ denotes the pairwise error probability between those two sequences and for AWGN channel with ML decoding is given by

$$\Pr\left(\check{\mathbf{t}}_d \left| \check{\mathbf{t}}_e\right.\right) = Q\left(\sqrt{\frac{d^2\left(\mathbf{q}(\check{\mathbf{t}}_d), \mathbf{q}(\check{\mathbf{t}}_e)\right)}{2N_0}}\right) \tag{2}$$

where $Q$ is the Gaussian complementary distribution function, $d = \left\|\mathbf{q}(\check{\mathbf{t}}_e) - \mathbf{q}(\check{\mathbf{t}}_d)\right\|$ is Euclidean distance between encoded signals at the place of the effect of Gaussian noise, and $N_0$ is the one-sided power spectral density. Equations (1) and (2) can be further rearranged [4] in order to get a relation between occurrence of Euclidean distances and their multiplicities

$$P(e) \leq \sum_{d_i \in \mathcal{D}} A_i Q\left(\sqrt{\frac{d_i^2}{2N_0}}\right). \tag{3}$$

The only two variables $\{A_i, d_i^2\}$ in (3) form an infinite set called distance spectrum of the code. Average first error event probability in (3) is often referred to as a frame error probability. Average bit and symbol error probabilities can be easily obtained from the frame error probability after enumeration of average number of bit or symbol errors along error paths with distances $d_i$. As an example, the union bound on bit error probability for trellis code becomes

$$P_b \leq \frac{1}{k}\sum_i B_i Q\left(\sqrt{\frac{d_i^2}{2N_0}}\right) \tag{4}$$

where $B_i$ is the average number of bit errors on error paths with distances $d_i$, and $k$ is the number of bits per symbol.

## 2.1 FSM Representation of Error Event

The enumeration of a distance spectrum is always done through an exhaustive search among all pairs of sequences that comply with individual first error events. However, the finite trellis assumption predetermines the application of finite state machine theory in error events evaluation [6]. The problem can be projected as sequences of transitions in an encoder and optimal decoder, that have essentially identical FSM description (Fig. 1) [7].

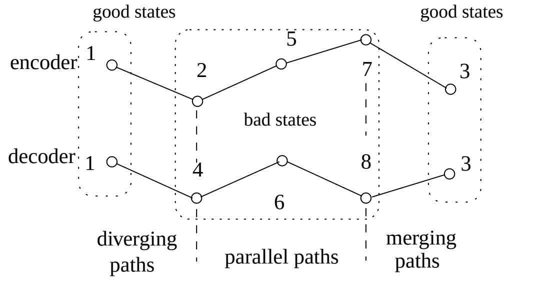


**Fig. 1.** The correct path in the encoder and the error path in the decoder of length 4.

Without regard to transition labels both FSMs are completely described by their state transition matrices (STM) $\mathbf{S}_e$ and $\mathbf{S}_d$. For general ML decoding these matrices become the same. STM of multiple concatenated FSMs is Kronecker product of partial single ones. STM is a square matrix, in which each row correspond to current states and each column represents the next states. To evaluate an arbitrary operation between those paths, we must consider a new product FSM $\mathbf{S} = \mathbf{S}_e \otimes \mathbf{S}_d$ with a new set of product states $\sigma = (\sigma_e, \sigma_d)$. The operator $\otimes$ denotes the generalized Kronecker type product (GKP). This operator keeps combining function of Kronecker product, but generalizes the product operation for arbitrary elements. New $N_e^2 \times N_e^2$ product matrix (PM) $\mathbf{S}$ ($N_e$ is the number of encoder states) can provide arbitrary operations among all combination of encoder and decoder states in fact. From Fig. 1 it follows, that elements in $\mathbf{S}$ could be further partitioned into two sets, the *good* $\sigma_e = \sigma_d$ and the *bad* $\sigma_e \neq \sigma_d$ ones. The good ones become *correct*, if there are no parallel transitions in the trellis. Again, the *simple error event* is defined by series of transitions from good states through some bad ones and back to the good states. The brute force method for enumerating all such events is via a corresponding *product state transition diagram*. Without any state minimization process, its state complexity remains $N_e^2$ like a product matrix. Fortunately, FSM theory offers a simple method for an evaluation of all required events via matrix operations.

Let the product matrix be partitioned into the equivalent $\mathbf{G}$, diverging $\mathbf{D}$, parallel $\mathbf{P}$ and merging $\mathbf{M}$ components. Then the *transfer matrix* for all accumulated products of error events of the length $L$ become

$$\begin{array}{rcll} \mathbf{T}^{(L)} & = & \mathbf{G} & \text{for } L = 1 \\ \mathbf{T}^{(L)} & = & \mathbf{D}\,\mathbf{P}^{L-2}\,\mathbf{M} & \text{for } L \geq 2 \end{array}. \tag{5}$$

The partitioned product matrix can be easily found from the naturally ordered original one by the following reordering[1] of rows and columns

$$n = \begin{cases} i, & i = j; \\ i(N_e - 1) + N_e + j, & i > j; \\ i(N_e - 1) + N_e + j - 1, & i < j; \end{cases} \tag{6}$$

where $N_e$ is the number of encoder states, $i, j$ are state indexes of the encoder and the decoder and $n$ is product state label.

$$\begin{array}{c} \\ 00 \\ 01 \\ 10 \\ 11 \end{array} \begin{array}{c} \begin{array}{cccc} 00 & 01 & 10 & 11 \end{array} \\ \left(\begin{array}{cccc} 1 & \mathcal{D}^4\mathcal{I} & \mathcal{D}^4\mathcal{I} & 1 \\ \mathcal{D}^2 & \mathcal{D}^2\mathcal{I} & \mathcal{D}^2\mathcal{I} & \mathcal{D}^2 \\ \mathcal{D}^2 & \mathcal{D}^2\mathcal{I} & \mathcal{D}^2\mathcal{I} & \mathcal{D}^2 \\ 1 & \mathcal{D}^4\mathcal{I} & \mathcal{D}^4\mathcal{I} & 1 \end{array}\right) \end{array} \qquad \begin{array}{c} \\ 00 \\ 11 \\ 01 \\ 10 \end{array} \begin{array}{c} \begin{array}{cccc} 00 & 11 & 01 & 10 \end{array} \\ \left(\begin{array}{cccc} 1 & 1 & \mathcal{D}^4\mathcal{I} & \mathcal{D}^4\mathcal{I} \\ 1 & 1 & \mathcal{D}^4\mathcal{I} & \mathcal{D}^4\mathcal{I} \\ \mathcal{D}^2 & \mathcal{D}^2 & \mathcal{D}^2\mathcal{I} & \mathcal{D}^2\mathcal{I} \\ \mathcal{D}^2 & \mathcal{D}^2 & \mathcal{D}^2\mathcal{I} & \mathcal{D}^2\mathcal{I} \end{array}\right) \end{array}$$

**Fig. 2.** Equivalent product matrices for two state simple TCM code from [8], left one with natural and right one with reordered mapping.

[1]As it was proved in [4] the ordering of states does not have an influence on transfer function analysis, provided that the rows and columns are ordered in the same manner.

It enables the partitioning of product transition matrix

$$\mathbf{S} = \begin{pmatrix} \mathbf{G}^{N_e,N_e} & \mathbf{D}^{N_e,N_e^2-N_e} \\ \mathbf{M}^{N_e^2-N_e,N_e} & \mathbf{P}^{N_e^2-N_e,N_e^2-N_e} \end{pmatrix} \tag{7}$$

where $N_e \times N_e$ matrix $\mathbf{G}$ denotes the matrix of correct transitions. The matrix $\mathbf{G}$ represents the same state transitions in an encoder as well as in an decoder state diagram. The superscript indexes denote the dimensions of individual submatrices. Fig. 2 shows two equivalent product matrices with natural and reordered mapping of rows and columns. It can be noticed at the sight of both matrices, that some rows and columns are the same. Their equivalence is potentially the first step in systematic state minimization process and demonstrates the level of linearity of the given system.

### 2.2 Transfer Function Bound

As an example we consider the problem of a bit error rate computation for a general code. The equation for a bit error probability is then given by [4]

$$P_b \leq \frac{1}{k}\sum_i \sum_{j=1}^{M} m_{i,j} d_{H_{i,j}} Q\left(\sqrt{\frac{d_i^2}{2N_0}}\right) \tag{8}$$

where $k$ is the number of information bits per symbol, $M$ is the number of terms with the same Euclidean distances $d_i^2$ and different Hamming distances $d_{H_{i,j}}$, and $m_{i,j}$ denotes their multiplicities. Because of numerical tractability [9], the classical formula for $Q$ function will be further replaced by its alternate finite integral equivalent

$$Q(x) = \frac{1}{\pi}\int_0^{\pi/2} e^{-\frac{x^2}{2\sin^2(\lambda)}} d\lambda. \tag{9}$$

The exact formula for $Q(x)$ is not in factorisable form and so it is often approximated by the simple exponential function $\frac{1}{\pi}e^{-\frac{x^2}{2}}$ at the expense of a suboptimal solution. Reformulation of the (9) using (8) gives

$$\begin{aligned} P_b &\leq \frac{1}{\pi k}\sum_i \sum_{j=1}^{M} \int_0^{\pi/2} m_{i,j} d_{H_{i,j}} e^{-\frac{d_i^2}{4N_0 \sin^2(\lambda)}} d\lambda \\ &= \frac{1}{\pi k}\int_0^{\pi/2} \frac{\partial}{\partial \mathcal{I}} \left[T\left(\mathcal{I}, \mathcal{D}(\lambda)\right)\right]\Bigg|_{\mathcal{I}=1, \mathcal{D}(\lambda)=e^{\frac{-1}{4N_0 \sin^2(\lambda)}}} d\lambda \end{aligned} \tag{10}$$

where

$$T\left(\mathcal{I}, \mathcal{D}(\lambda)\right) = \sum_i \sum_{j=1}^{M} m_{i,j} \mathcal{I}^{d_{H_{i,j}}} \mathcal{D}^{d_i^2}(\lambda) \tag{11}$$

represents the *transfer function* of a trellis code. To find all distances $d_i$ and $d_{H_{i,j}}$ of error events of length $L$, we can utilize a transfer matrix (5) (Sec. 2.1), where each entry $T_{m,n}$ in the matrix $\mathbf{T}_L$ represents all distances of length $L$ from product state $m$ to the product state $n$. We need not have defined an exact form of individual STMs $\mathbf{S}_e$, $\mathbf{S}_d$ except that both must contain a useful description of input-output relationship for given FSMs. In the case of TCM the input codeword and relevant constellation symbol for the given state transition are needed. Then the operation in generalized Kronecker type product combines these quantities to incremental distances among all transitions in the encoder and all transitions in the decoder at one time unit. Provided that there are no parallel transitions, one non-zero entry of the matrix $\mathbf{S}$ is

$$S_{m,n} = \frac{1}{2^k}\mathcal{I}^{d_H(m,n)} \mathcal{D}(\lambda)^{d^2(m,n)}. \tag{12}$$

If the transitions are not allowed, the entry associated with this transition becomes zero. Since there is only one correct transition at any time, the factor $1/2^k$ represents its probability.

The distances associated with all error events are found via adding over their lengths

$$\mathbf{T}\left(\mathcal{I}, \mathcal{D}(\lambda)\right) = \mathbf{G} + \sum_{l=2}^{\infty} \mathbf{T}^{(l)} = \mathbf{G} + \sum_{l=2}^{\infty} \mathbf{D}\mathbf{P}^{(l-2)}\mathbf{M}. \tag{13}$$

An alternative equivalent expression for the transfer function then becomes

$$T\left(\mathcal{I}, \mathcal{D}(\lambda)\right) = \frac{1}{N_g}\sum_i \sum_j T_{i,j}\left(\mathcal{I}, \mathcal{D}(\lambda)\right) \tag{14}$$

where $T_{i,j}$ are individual components of the transfer function matrix.The factor $1/N_g$ represents the initial probability of beginning at any good states, which is assumed to be the same for all $N_g$ good product states. Without any state minimization process the $N_g$ is equal to $N_e$. To ensure the applicability of the transfer function based on the transfer matrix evaluation, the probability of pairwise error event in (10) should be in a product form of elements, which correspond to increments of distances. The transfer function in (14) is equivalent to (11), and therefore we can extract the relevant multiplicities from (14) in order to obtain the distance spectrum $\left\{\sum_{j=1}^{M} m_{i,j} d_{H_{i,j}}, d_i^2\right\}$. The exhaustive search method for the distance spectrum enumeration was replaced here by the simple matrix multiplication in fact.

## 3. Extended Transfer Bound

In the following subsection we propose an extension of transfer bound, which solves the problem of exact performance analysis in a presence of a communication channel [2].

### 3.1 Parametric Channel

In the presence of a channel parameter, the error event probability depends on channel nuisance parameters $\theta$ and their estimates $\hat{\theta}$. Random ones could be eliminated out via averaging over their distributions

$$P(e) = \int_{\theta}\int_{\hat{\theta}} P\left(e;\theta,\hat{\theta}\right) p\left(\theta,\hat{\theta}\right) d\theta d\hat{\theta}. \quad (15)$$

The problem of performance analysis is to find a suitable expression for a pairwise error event probability, which not only satisfies transfer bound constraints, but also allows elimination of nuisance parameters. As we have shown above, it is not satisfied for non-ergodic continuous random parameter process. We believe that one way out lies in establishing of the discrete nuisance parameter space [10] and joining it with the state space made by product FSM. Let us consider that the nuisance parameter is a mixture of two random processes—an independent identically distributed (IID) continuous-valued one and the discrete one

$$\theta_n = \phi_n + \vartheta_n \quad (16)$$

where $\vartheta_n$ expresses the random IID fast parameter fluctuation, and $\phi_n$ is modeled in order to account for time correlations. Let $\phi_n$ be modeled by the discrete-time stationary Markov chain [11], which outputs the values from the finite space $\phi_n \in \{\phi_0,\phi_1,...,\phi_{\mathcal{Q}-1}\}$, where $\mathcal{Q}$ is the number of quantization levels and $\phi_k = \Phi_k(\theta)$ is the $k$-th quantization interval. It was shown in [12][13] that such model is mostly sufficient for modeling of channel phase and fading amplitude considering their realistic dynamics. The component $\vartheta_n$ describes the statistical behavior inside the quantization interval and is modeled as the IID process. The composite model is trying to separate the random behavior of the original parameter into two components $\phi_n$ and $\vartheta_n$, meeting the requirements of error analysis at the cost of an approximate solution.

For the simplicity of the evaluation we consider a $\mathcal{Q}$ state first-order Markov model for a nuisance parameter and we are conscious of its limitation in modeling of statistical behavior for a given parameter [12]. The first-order Markov chain is defined by its $\mathcal{Q}\times\mathcal{Q}$ transition probability matrix $\mathbf{B}$, where each entry corresponds to individual transition probabilities $b_{i,j} = P(\check{\phi}_n=\phi_j | \check{\phi}_{n-1}=\phi_i)$ and the vector of the initial state distribution $\Pi = \left[\pi_{\check{\phi}_0=\phi_1},\pi_{\check{\phi}_0=\phi_2},...,\pi_{\check{\phi}_0=\phi_{\mathcal{Q}-1}}\right]$. For the unknown continuous parameter $\theta$ the general average error probability is given by

$$\begin{aligned} P(e) &= \int_{\theta}\sum_{L}\sum_{\mathbf{e}_L}\Pr\left(\mathbf{e}_L;\theta\right)p\left(\theta\right)d\theta \quad (17)\\ &= \sum_{L}\sum_{\mathbf{e}_L}\int_{\theta}\Pr\left(\mathbf{e}_L;\theta\right)p\left(\theta\right)d\theta \end{aligned}$$

where $\mathbf{e}_L$ is the vector of all length $L$ error events. For better understanding we found more convenient to show the elimination process directly on the error event probability evaluation.

Let us assume that $\phi_n = 0$ and the probability of pairwise error event $\Pr(\mathbf{e}_L;\vartheta_L) = \prod_{n\in L}\Pr(e_n;\vartheta_n)$ is factorisable process. Then the $\theta_n = \vartheta_n$ is the IID parameter and the multidimensional integral in (17) collapses into the multiplication of single dimensional ones

$$\begin{aligned} \Pr(\mathbf{e}_L) &= \int_{\vartheta}\Pr\left(\mathbf{e}_L;\vartheta_L\right)p\left(\vartheta_L\right)d\vartheta_L\\ &= \prod_{n\in L}\int_{\vartheta_n}\Pr\left(e_n;\vartheta_n\right)p\left(\vartheta_n\right)d\vartheta_n \quad (18)\end{aligned}$$

It means, that the continuous IID part of $\theta_n$ can be easily eliminated from the pairwise error probability and then such operation also satisfies the fundamental limits of transfer bound. The parameter $\phi_n$ fluctuation is assumed to be slow enough that its actual value can be assumed to as constant for time duration of a channel symbol. The elimination of the finite state component of given length $L$ is easily obtained as

$$\begin{aligned} \Pr(\mathbf{e}_L) &= \sum_{\check{\phi}_0=\phi_1}^{\phi_{Q-1}}\pi_{\check{\phi}_0}\sum_{\check{\phi}_L}\prod_{n=1}^{L}\Pr\left(e_n;\check{\phi}_n\right)b_{\check{\phi}_{n-1},\check{\phi}_n}\\ &= \Pi\left[\prod_{n=1}^{L}\mathbf{E}(e_n)\right]\mathbf{1}^T \quad (19)\end{aligned}$$

where the operator $\sum_{\check{\phi}_L}$ realizes summation over all possible $Q^L$ product terms, and $\mathbf{\Pi}$ is the vector of the parameter initial state distribution. Elements in matrix $\mathbf{E}(e_n)$ are time increments of pairwise error event, that vary depending on parameter state transition (Fig. 3). Random IID process is eliminated according to its parameter distribution at each quantized interval

$$\mathbf{E}(e_n)_{i,j} = \int_{\Phi_j^{-1}(\phi_j)}\Pr\left(e_n;\vartheta\right)p(\vartheta|\,\phi_j)d\vartheta b_{\phi_i,\phi_j} \quad (20)$$

where $p(\vartheta|\,\phi_j)$ denotes the parameter state conditional probability density function and the integration interval is defined over the quantization interval associated with the given $\phi_j$. The average error event probability is then

$$P(e) = \sum_{L}\sum_{\mathbf{e}_L}\Pi\left[\prod_{n\in\mathbf{e}_L}\mathbf{E}(e_n)\right]\mathbf{1}^T \quad (21)$$

where $n \in \mathbf{e}_L$ represents series of $n$, which correspond to the given error event $\mathbf{e}$.

Recall from Section 2.1 that each error event can be represented as a path in an error state diagram. We have defined a product state and transfer FSM as generalized Kronecker type product of two encoder FSMs. The elements of transfer matrix correspond to all accumulated products of error events of the given length $L$. Our goal is to find a new form of a transfer function and its components, which also account for averaging over a nuisance parameter. The computation of union bound corresponds to the elimination of simple pairwise error events from the full error space and such process can be joined together with the elimination of the finite state parameter.

Now, we utilize the equivalence between the increment of the pairwise error event in (18) and (19) and the product matrix element in transfer function bound (12), which is made by integral representation of the $Q$ function. This will enable us to form new PM compounded of code PM and $\mathbf{E}(e_n)$ through the generalized Kronecker type product. Product operation corresponds to error dependent elimination process mentioned above in (20). According to (19) and (12) we propose the new *extended product transition matrix* $\mathbf{S}^{\mathbf{E}}$ which allows the entries to be sub-matrices

$$S^{\mathbf{E}}_{m,n,(i,j)} = p \sum_{\text{parallel}} E_{\vartheta|\phi_j}\left[\mathcal{D}^{d^2_{m,n}(\vartheta)}\right]\mathcal{I}^{d^{\text{Ham}}_{m,n}} b_{\phi_i,\phi_j} \quad (22)$$

where $p = p\left(\sigma_{n-1} \to \sigma_n \left|\sigma_{n-1}\right.\right)$ is the correct transition probability, $\sum_{\text{parallel}}$ is the sum over all possible parallel transitions, $d^2_{m,n}$ is the distance of useful signals of correct and erroneous detected symbols, and $d^{\text{Ham}}_{m,n}$ is the Hamming distance of corresponding input symbols. The extended transfer function is created by partitioning of $\mathbf{S}^{\mathbf{E}}$ over $m, n$ indexes of sub-matrices. The joint initial probability vector now combines both the probability of being at any good product state and $\mathbf{\Pi}$ as $\mathbf{\Pi}^{\mathbf{E}} = \frac{1}{N_g}\left[\mathbf{\Pi}_1, \mathbf{\Pi}_2, ..., \mathbf{\Pi}_{N_g}\right]$. The expression for the extended transfer function then becomes

$$T\left(\mathcal{I},\mathcal{D}\right)^E = \mathbf{\Pi}^{\mathbf{E}}\mathbf{G}^{\mathbf{E}}\mathbf{1}^T_{N_gQ} + \sum_{l=2}^{\infty}\mathbf{\Pi}^{E}\mathbf{D}^{\mathbf{E}}\mathbf{P}^{\mathbf{E}(l-2)}\mathbf{M}^{\mathbf{E}}\mathbf{1}^T_{N_gQ} \quad (23)$$

where $\mathbf{G}^{\mathbf{E}}, \mathbf{D}^{\mathbf{E}}, \mathbf{P}^{\mathbf{E}}, \mathbf{M}^{\mathbf{E}}$ are individual components of the matrix $\mathbf{S}^{\mathbf{E}}$ (Sec. 2.1).

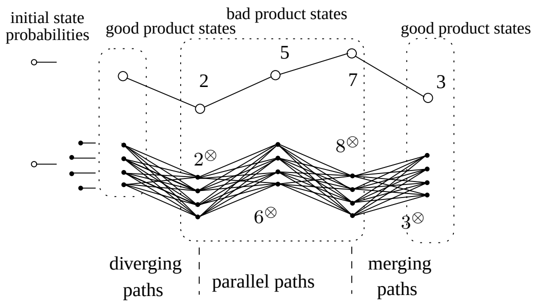


**Fig. 3.** The difference between error events produced by extended and former product FSMs.

This concept is illustrated in Fig. 3, where the difference between former and extended error events are depicted. Extended ones allow for averaging of the nuisance parameter over all length former error event.

### 3.2 State Space Parameter Modeling

In the following paragraph we only pick out the method to gain essential characteristics of the first-order Markov chain. In such a case we can follow the simple analytical approach, where initial state probabilities are given by

$$\pi_k = \int_{\Phi_k^{-1}(\phi_k)} p\left(\theta\right) d\theta \quad (24)$$

where $\pi_k$ satisfies $\sum_{k=1}^{Q}\pi_k = 1$. Quantization intervals contrary to $p\left(\theta\right)$ are often defined on finite parameter span, which conflicts with the unity condition and it can be solved by the following normalization $\tilde{\pi}_k = \pi_k / \sum_{k=1}^{Q}\pi_k$. The quantization intervals can be chosen uniformly over a parameter set or in such a way that the initial state probabilities of all states become the same. In the second case we need not compute initial state distribution. The transition probability matrix of the model has stationary transition probabilities

$$b_{i,j} = \frac{\int_{\Phi_j^{-1}(\phi_j)}\int_{\Phi_i^{-1}(\phi_i)} p\left(\theta_{n-1},\theta_n\right) d\theta_{n-1} d\theta_n}{\int_{\Phi_i^{-1}(\phi_i)} p\left(\theta_{n-1}\right) d\theta_{n-1}} \quad (25)$$

where $p\left(\theta_{n-1},\theta_n\right)$ is bivariate PDF of two successive samples of the parameter time process. As in (24) the transition probability matrix can be adjusted in such a way that the rows sum to one $\tilde{b}_{i,j} = b_{i,j} / \sum_{j=1}^{Q}\pi_{i,j}$.

# 4. Applications

In the following subsection, we shall describe an application of proposed principles on performance evaluation of a real communication system.

### 4.1 Bit Error Rate Performance for Rayleigh Fading Channel—Known Channel State Information

A modulated signal is passed through the channel with AWGN and unknown nuisance parameters with the vector model

$$\mathbf{x} = \sqrt{2E_s}\,\text{diag}\left[\mathbf{g}\right]\mathbf{q} + \omega \quad (26)$$

where $g_n = \alpha_n e^{j\varphi_n}$, $\alpha_n$, $\varphi_n$ are the sampled channel amplitude and phase, $\mathbf{q}$ is the vector of channel symbols, and $\omega$ is the vector of zero mean complex Gaussian random variables with the variance $E\left[\left|\omega_n\right|^2\right] = 2N_0$.

For the known channel state information the pairwise error probability is given by [8]

$$\Pr\left(\check{\mathbf{t}}_i\left|\check{\mathbf{t}}_k\right.\right) = \frac{1}{\pi}\int_0^{\pi/2} E_\theta\left[\prod_{n\in L}\mathcal{D}\left(\lambda\right)^{\theta_n^2\|\triangle q_n\|^2}\right] d\lambda \quad (27)$$

where $\theta_n = \alpha_n$ denotes a channel amplitude sample and $\triangle q_n$ is the channel symbol difference of $i$-th and $k$-th message. For $\theta_n$ IID process, the expectation operator get through the product of independent elements, which will only influence the determination of the product state matrix in the standard transfer bound computation by the elimination of the parameter from its individual elements. The fundamental question was how to interpret all components of extended transfer bound for the mixture parameter defined in (16) (the conditional probability density function $p(\vartheta|\,\phi_j)$ and Markov chain characteristics $\mathbf{\Pi}$ and $\mathbf{B}$). Two main goals was determined in proper characteristics evaluation. The first one is a closeness of a statistical behavior of the composite parameter to the original one, and the second one is identical analytical results of the original and extended transfer bound for the random IID channel parameter.

The elimination of the the IID part can be done over an original parameter distribution at regular quantized intervals. The conditional probability density function $p(\vartheta|\,\phi_j)$ is defined as in Fig. 4 and the two consecutive samples of $\theta_{n-1}$ and $\theta_n$ are assumed to have bivariate Rayleigh distribution with the correlation coefficient $\rho = |J_0\left(2\pi f_D T_p\right)|$ (uniform variance of component Gaussian processes)

$$\begin{aligned} p\left(\theta_{n-1},\theta_n\right) &= \tfrac{1}{\sigma^2(1-\rho^2)}\theta_{n-1}\theta_n e^{-\frac{1}{2\sigma(1-\rho^2)}\left(\theta_{n-1}^2+\theta_n^2\right)} \times \\ &\times \quad I_0\left(\tfrac{\rho}{\sigma(1-\rho^2)}\theta_{n-1}\theta_n\right) \end{aligned} \tag{28}$$

where $f_D$ is the Doppler frequency and $T_p$ is the sample period.

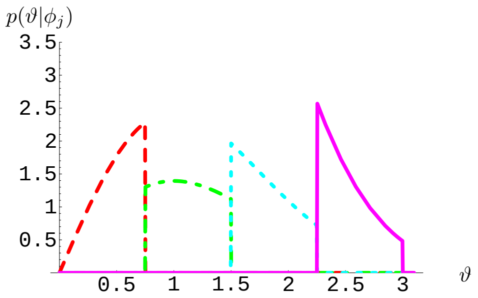


**Fig. 4.** Figure shows the behavior of conditional probability density functions for $\vartheta_n$ IID parts, four quantization intervals and Rayleigh distribution.

Acquired Markov characteristics are substituted into the (22) in order to get extended transfer function (23). The actual extended transfer function can be utilized in the same way as in (10)

$$P_b \leq \frac{1}{\pi}\int_0^{\pi/2}\left[\frac{1}{k}\,\frac{\partial}{\partial \mathcal{I}}T\left(\mathcal{I},\mathcal{D}(\lambda)\right)^E\Big|_{\mathcal{I}=1}\right]d\lambda. \tag{29}$$

## 4.2 Bit Error Rate Performance for Non-Ideal Coherent Detection

In this case the detector metric does not take into account the error of an estimated parameter and perfect synchronization is expected. The suitable form of the exact pairwise error probability for phase is still not available and can be mostly bounded by Chernoff approximation. In our case the Chernoff bound results in

$$\begin{aligned} \Pr\left(\check{\mathbf{t}}_i\,|\check{\mathbf{t}}_k,\theta\right) &\leq e^{-\nu\mathrm{Re}\left[\sqrt{2E_s}(\triangle\mathbf{q})^H\mathrm{diag}\left[e^{j\theta}\right]\mathbf{q}^{(k)}\right]}\times \\ &\times \quad E\left[e^{-\nu\mathrm{Re}\left[(\triangle\mathbf{q})^H\mathrm{diag}\left[e^{-j\hat{\varphi}}\right]\omega\right]}\right] \end{aligned} \tag{30}$$

where $\triangle\mathbf{q} = \left(\mathbf{q}^{(k)} - \mathbf{q}^{(i)}\right)$ is the difference between the incorrect path $\mathbf{q}^{(i)}$ and the correct path $\mathbf{q}^{(k)}$, $\theta = \varphi - \hat{\varphi}$ is difference between channel and estimated phase [2]. The Chernoff parameter $\nu$ should be optimized in order to get the most tightest upper bound. Since $\mathrm{Re}\left[(\triangle\mathbf{q})^H\,\mathrm{diag}\left[e^{-j\hat{\varphi}}\right]\omega\right]$ is the sum of Gaussian random variables each with zero mean and variance $N_0\left\|q_n^{(k)} - q_n^{(i)}\right\|^2$, the expectation over right hand side of Chernoff bound then becomes

$$E\left[e^{-\nu\mathrm{Re}\left[(\triangle\mathbf{q})^H\mathrm{diag}\left[e^{-j\hat{\varphi}}\right]\omega\right]}\right] = \prod_n e^{\nu^2 N_0\left\|q_n^{(k)}-q_n^{(i)}\right\|^2/2}. \tag{31}$$

For any value of $\nu$ the equation (30) gives an upper bound. In our case we chose the suboptimal one $\nu_0 = \sqrt{2E_s}/2N_0$ instead of the complicated analytical solution for the following reasons. For the first the resulting bound can be written in term of distance increments and for $\theta_n = 0$ these increments correspond to Euclidean distances between channel symbols. We have also verified that our bound is able to follow correct error performance for phase variances $\sigma_\theta^2 < 0.2$.

The squared distance in the product state matrix element then becomes

$$\begin{aligned} \xi(\psi_n^{(k)},\psi_n^{(i)},\theta_n) &= -2\left[1-\cos\left(\psi_n^{(k)}-\psi_n^{(i)}\right)\right] \\ &+4\left(-\cos\left(\psi_n^{(k)}-\psi_n^{(i)}+\theta_n\right)+\cos\left(\theta_n\right)\right) \end{aligned} \tag{32}$$

where $\psi_n^{(k)}$, $\psi_n^{(i)}$ are the angles of transmitted and estimated channel symbols. The upper bound on pairwise error probability written in terms of transfer bound results in

$$\Pr\left(\check{\mathbf{t}}_i\,|\check{\mathbf{t}}_k\right) = E_\theta\prod_{n\in L}\left[\mathcal{D}^{\xi(\triangle\mathbf{q},\theta_n)}\right] \tag{33}$$

where each product state matrix element is parametrized with an unknown phase error and $\mathcal{D} = e^{-\frac{E_s}{4N_0}}$. The Markov model characteristics could be obtained in the same way as for the Rayleigh fading process in the previous paragraph. However in the random phase error case two consecutive samples are assumed to have the Gaussian bivariate distribution with the known variance and correlation coefficient.

## 4.3 Simulation Results

In this section, some simulation results are presented to illustrate the correctness of the proposed algorithm. We have simulated the performance of two rate $1/2$ Ungerboeck trellis codes, one with two states and one with four states [8] both with QPSK mapping (Figs. 5, 6).

### 4.3.1 Rayleigh Fading Channel

The channel fading is modeled as a mixture of four state quantized and IID processes, where $p(\vartheta|\phi_j)$ is defined as in Fig. 4. We also noticed that the correctness of the analytical performance at low SNR highly depends on the distance spectrum of the code we have used.

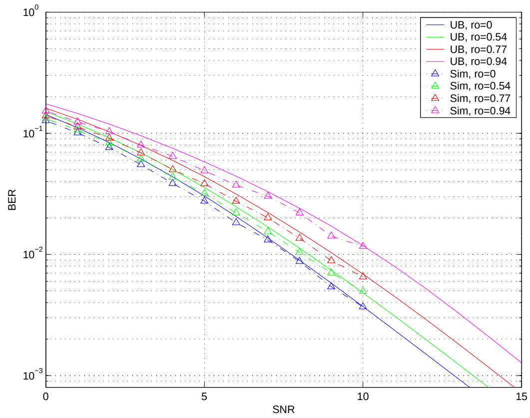


**Fig. 5.** Analytical performance versus simulation of two state trellis code for various correlation coefficient $\rho$. The Bit Error Rate as a function of Signal to Noise Ratio. Simulation curves are tagged by triangles.

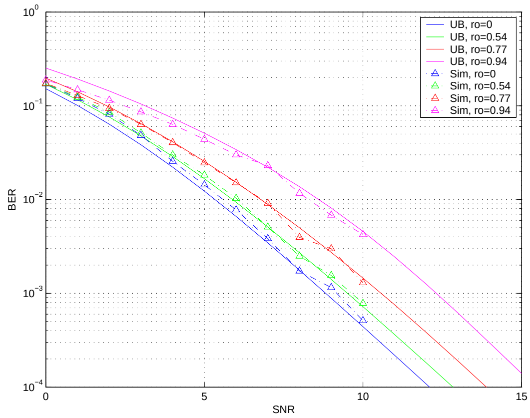


**Fig. 6.** Analytical performance versus simulation of four state trellis code for various correlation coefficient $\rho$.

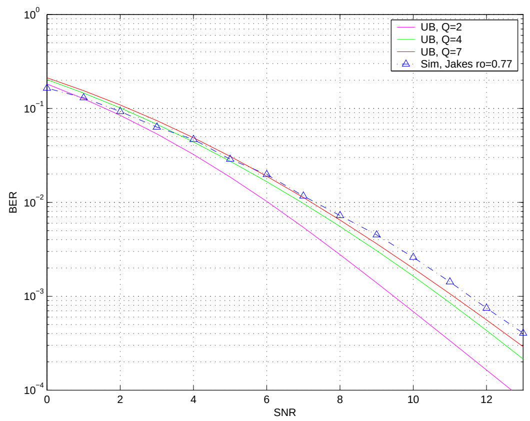


**Fig. 7.** Error performance results of the four state TCM for different number of quantization intervals (states) versus simulated performance made by Jakes simulator for identical correlation coefficient.

For the four state one the spectrum begins at higher distances and the union bound approximation has lesser influence on the analytical performance evaluation. In the simpler code case the correct asymptotic behavior at low SNRs was reached by shortening of the maximum length of examined error events. Another problem we are interested in is how accurate our analytical results based on the mixture parameter model correspond to the error performance of the system with a real fading. Fig. 7 shows the dependence of the error performance on the number of quantization intervals and compares both the analytical results and error measure of the system with a channel amplitude generated by the Jakes fading simulator. From these curves we see that for a limited number of quantization intervals we can get nearly correct error performance asymptotes ranging from low to mid values of SNR.

### 4.3.2 Phase Synchronization Error

In the second example the phase synchronization error is modeled as a mixture of six state quantized and IID processes. The conditional probability density function $p(\vartheta|\phi_j)$ and Markov chain characteristics are defined from Gaussian distribution. Fig. 8 compares the real simulated performance and Chernoff bound for two different correlation coefficients.

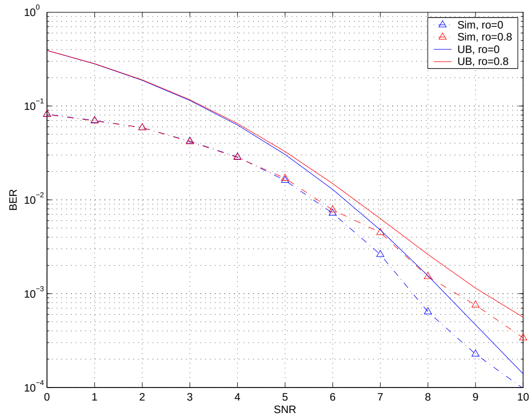


**Fig. 8.** Chernoff bound versus simulation of two state trellis code for phase error with $\sigma_\theta = 0.4$ and two different correlation coefficient $\rho$. The Bit Error Rate as a function of Signal to Noise Ratio. Simulation curves are tagged by triangles.

## 5. Conclusion

We established the general framework for the performance analysis of the ordinary finite memory encoder and the decoder under correlated continuous valued channel parameter assumption. We have shown that our analytical solution correctly follows the results obtained by the computer simulation of the same communication system. Our extended transfer bound is able to predict the nearly correct error performance asymptotes of the system in Rayleigh fading channel. From FSM theory point of view our proposal extends the existing principles in a general theoretical level and can be easily utilized in any other application.

## Acknowledgements

The work was supported by Grant Agency of the Czech Republic, grant 102/05/2177, IG CTU0507813, and by the Ministry of education, youth and sports of the Czech Republic, grant OC273 and prog. MSM6840770014.

## References


[1] VCELAK, J., SYKORA, J. Extended Transfer Bound Error Analysis in the Presence of Channel Random Nuisance Parameter. In *Proc. IEEE Int. Symp. on Personal, Indoor and Mobile Radio Communications (PIMRC)*. Berlin(Germany), Sep 2005.

[2] VCELAK, J., SYKORA, J. Analytical Error Performance Analysis for Reduced Complexity Detection of General Trellis Code with Parametric Uncertainty. *COST#273 [CD-ROM], TD-04-132*. Gothenburg(Sweden), Jun 2004, p. 1 – 5.

[3] SYKORA, J. *Theory of Digital Communication*. Lecture notes, CTU FEE Prague. 2001.

[4] ZHANG, W. *Finite State System in Mobile Communication*. PhD Thesis, University of South Australia. 1996.

[5] CHUGG, K., ANASTASOPOULOS, A., CHEN, X. *Iterative detection, Adaptivity, Complexity Reduction and Applications*. Kluwer Academic Publishers, 2001.

[6] BIGLIERI, E. High-Level Modulation and Coding for Nonlinear Satellite Channels. *IEEE Trans. on Comm.* May 1984, no. 5.

[7] SCHLEGEL, CH. B., PEREZ, L. C. *Trellis and Turbo Coding*. John Wiley & Sons, Inc., 2004.

[8] SIMONS, M., ALOUINI, M. *Digital Communication over Fading Channels: A Unified Approach to Performance Analysis*. John Wiley & Sons, 2000.

[9] SIMONS, M., ALOUINI, M. A Unified Approach to the Performance Analysis of Digital Communication over Generalized Fading Channels. In *IEEE Proceedings*. Sep 1998, p. 1860 – 1877.

[10] NASSAR, C. R., SOLEYMANI, M. R. Application of Quantization Theory to Data Detection in a Presence of Nuisance Parameters. *IEEE Trans. on Communication*. June 1999, vol. 47, no. 6.

[11] EPHRAIM, Y., MERHAV, N. Hidden Markov Processes. *Trans. on Inf. Theory*. June 2002, vol. IT-48, no. 6, p. 1518 – 1568.

[12] TURIN, W., NOBELEN, R. Hidden Markov Modeling of Flat Fading Channel. *IEEE Journal on Sel. Areas in Comm*. Dec 1998, vol. 16, no. 9, p. 1809 – 1817.

[13] KOMNINAKIS, CH., WESEL, R. D. Joint Iterative Channel Estimation and Decoding in Flat Correlated Rayleigh Fading Channel. *Journal on Sel. Areas in Comm*. Sep 2001, vol. 19, no. 9, p. 1706 – 1717.


## About Authors . . .

**Jan VČELÁK** received his Ing. degree from the Czech Technical University in Prague in 2002. Currently he is a PhD student at the Department of Radioelectronics of the same university. His research is mainly focused on advanced detection, synchronization and equalization techniques for spatial diversity communication systems.

**Jan SÝKORA** is associate professor at the Czech Technical University in Prague, Faculty of Electrical Engineering, Department of Radioelectronics. His research interest spans the whole area of the digital communication theory, including modulation, coding, synchronization, equalization and detection. Currently he focuses mainly on adaptive and spatial diversity communications.